

Article

Predicting the Splitting Tensile Strength of Recycled Aggregate Concrete Using Individual and Ensemble Machine Learning Approaches

Yongzhong Zhu ^{1,*}, Ayaz Ahmad ^{2,3,*} , Waqas Ahmad ² , Nikolai Ivanovich Vatin ⁴ ,
Abdeliazim Mustafa Mohamed ^{5,6}  and Dina Fathi ⁷

- ¹ Hunan Institute of Technology, School of Design and Art, Hengyang 421001, China
² Department of Civil Engineering, COMSATS University Islamabad, Abbottabad 22060, Pakistan; waqasahmad@cuiatd.edu.pk
³ MaREI Centre, Ryan Institute and School of Engineering, College of Science and Engineering, National University of Ireland, H91 TK33 Galway, Ireland
⁴ Peter the Great St. Petersburg Polytechnic University, 195291 St. Petersburg, Russia; vatin@mail.ru
⁵ Department of Civil Engineering, College of Engineering in Al-Kharj, Prince Sattam bin Abdulaziz University, Al-Kharj 11942, Saudi Arabia; a.bilal@psau.edu.sa
⁶ Building & Construction Technology Department, Bayan College of Science and Technology, Khartoum 210, Sudan
⁷ Structural Engineering and Construction Management Department, Faculty of Engineering and Technology, Future University in Egypt, New Cairo 11845, Egypt; dinamohamed@fue.edu.eg
* Correspondence: zyzfrq@126.com (Y.Z.); ayazahmad@cuiatd.edu.pk (A.A.)



Citation: Zhu, Y.; Ahmad, A.; Ahmad, W.; Vatin, N.I.; Mohamed, A.M.; Fathi, D. Predicting the Splitting Tensile Strength of Recycled Aggregate Concrete Using Individual and Ensemble Machine Learning Approaches. *Crystals* **2022**, *12*, 569. <https://doi.org/10.3390/cryst12050569>

Academic Editors: Nichola Coleman and Samantha E. Booth

Received: 21 February 2022

Accepted: 15 April 2022

Published: 19 April 2022

Publisher's Note: MDPI stays neutral with regard to jurisdictional claims in published maps and institutional affiliations.



Copyright: © 2022 by the authors. Licensee MDPI, Basel, Switzerland. This article is an open access article distributed under the terms and conditions of the Creative Commons Attribution (CC BY) license (<https://creativecommons.org/licenses/by/4.0/>).

Abstract: The application of waste materials in concrete is gaining more popularity for sustainable development. The adaptation of this approach not only reduces the environmental risks but also fulfills the requirement of concrete material. This study used the novel algorithms of machine learning (ML) to forecast the splitting tensile strength (STS) of concrete containing recycled aggregate (RA). The gene expression programming (GEP), artificial neural network (ANN), and bagging techniques were investigated for the selected database. Results reveal that the precision level of the bagging model is more accurate toward the prediction of STS of RA-based concrete as opposed to GEP and ANN models. The high value (0.95) of the coefficient of determination (R^2) and lesser values of the errors (MAE, MSE, RMSE) were a clear indication of the accurate precision of the bagging model. Moreover, the statistical checks and k-fold cross-validation method were also incorporated to confirm the validity of the employed model. In addition, sensitivity analysis was also carried out to know the contribution level of each parameter toward the prediction of the outcome. The application of ML approaches for the anticipation of concrete's mechanical properties will benefit the area of civil engineering by saving time, effort, and resources.

Keywords: concrete; recycled aggregate; environment-friendly material; splitting tensile strength; machine learning

1. Introduction

The splitting tensile strength of concrete is an important mechanical property that significantly affects the quantity and size of cracking in concrete structures [1]. Due to the fact that concrete is a weak material in tension, it is necessary to conduct a pre-evaluation of its split-tensile strength [2]. The splitting tensile strength (STS) of concrete is related to a variety of mechanical and durability parameters directly or indirectly [3–5]. Flexural strength is another critical attribute to consider when building structural concrete since it affects the concrete's flexural cracking, shear strength, deflection properties, and brittleness ratio [6–10]. Mechanical characteristics of recycled aggregate concrete (RAC) are dependent

on a variety of elements, including the physical properties of the recycled aggregate utilized and the resulting matrix's microstructure [5,11]. RAC typically has less strength than natural aggregate concrete because of poor bonding between the aggregate and the old mortar, fractures, and fissures in the recycled aggregate caused by the recycling process, and the existence of low-permeability mortar attached to the recycled aggregate [12–14]. The strength of RAC is dependent on the recycled aggregate replacement ratio, water–cement ratio (w/c), recycled aggregate moisture content, and the physical and mechanical properties of the recycled aggregate [15–19]. When w/c is maintained constant, experimental evidence indicates that recycled aggregate replacement content has a substantial effect on the strength of RAC [20–25]. When natural aggregate is completely replaced by recycled aggregate, RAC's compressive strength can be reduced by up to 30% [26–28].

Concrete makes up the lion's share of construction and demolishing waste and is the most apparent component [29,30]. As the contemporary industry continues to flourish, numerous types of industrial solid wastes have become a burden on society and the environment [31,32]. One of the most effective recycling methods is to employ certain solid wastes as supplemental cementitious materials (SCMs) in the manufacture of cement-based materials [33–35]. The most important, available in a large amount, and easy to use is recycled aggregate [36,37]. However, evaluating and managing the geometry of RCA is crucial for its successful implementation in novel concrete applications [38]. Gradation is the most critical attribute that practitioners and scholars consider [39–42]. Although shape and texture criteria are visually checked on occasion, they are not used to drive the actual mix design [43,44]. Indeed, aggregate shape and texture are critical properties that influence paste demand, workability, and strength [45,46]. Sphericity, flatness, angularity, and roundness are the primary characteristics associated with the shape [47,48].

Since the precise source and age of RCA are frequently unknown, it is necessary to create a testing process that adequately characterizes RCA for its numerous potential applications [49]. While RCA is more challenging than the natural aggregate (mainly because of the remaining mortar percentage), current characterization efforts are concentrated on gradation, specific gravity, and absorption in various specifications [50,51]. Similarly, obtaining the required strength of concrete normally needs some time in days [52,53]. Numerous analytical models have been created for the prediction of strength based on numerous assumptions about the process, equilibrium development, and deformation compatibility [54–63]. The use of ML approaches to predict the strength of selected concrete is gaining more popularity as it initially forecasts the required outcome without consuming time, cost of the experimental approach, and physical effort [64–69]. Shahmansouri et al. [2] predicted the C-S containing SCM using GEP. The proper correlation was reported in the study between the experimental and predicted results. Lee et al.'s [70] research was based on the use of the ANN technique for the prediction of concrete strength, which describes that the I-PreConS using ANN shows impressive results toward the prediction. Sharafati et al.'s [71] research was based on the application of bagging ensemble algorithm anticipation of the C-S of a hollow concrete masonry prism. The result indicates that the BR was more defective than the SVR regressor. Han et al. [72] examined the performance of ensemble ML approaches for the modulus of elasticity of RA. The ensemble machine learning model regularly outperforms many standalone machine learning models in terms of prediction performance.

This research describes the performance comparison of the various ML techniques toward the prediction of the STS of RA concrete. It was clear from the coefficient of determination (R^2) value that the BR has a high precision level for predicting the STS of concrete as opposed to the GEP and ANN ML approaches. Machine learning methods require a dataset, which may be gathered from previous studies, as several investigations have been conducted to determine the material strength. The data collection can then be used to train machine learning models and forecast material qualities. This research will be helpful to researchers in selecting the best ML approach for the prediction purpose.

2. Methods

2.1. Database Description

The database used in this study to run the selected models for predicting the STS of RA concrete was taken from the literature [73–89]. Python coding helps to run the employed models. Input parameters (total 9) such as cement, fine aggregate, natural coarse aggregate (NCA), water, recycled coarse aggregate (RCA), the maximum size of RA, superplasticizers, the density of RA, and water absorption of RA with a single output parameter (STS) were used to run the models. A total of 166 data points were used to run the selected models. A total of 60% of the data were allocated for the training set, 20% for testing, and 20% for validation purposes. Table 1 illustrates the statistical analysis of variables, illustrating the numerous mathematical descriptions of input values. Figure 1 depicts the relative frequency distributions of the nine variables. Additionally, the step-by-step procedure of the adopted methods and the research approach is presented in the form of a flowchart, as illustrated in Figure 2, which contains information about the study's stepwise procedure. The data set used for running the models has been added as a Supplementary Material with the file name of Data set.

Table 1. Descriptive investigation of the input parameters.

Variables	*W	*C	*F-A	NCA	RCA	SP	Size	Density	*WA
Mean value	180.38	364.42	688.47	382.02	656.69	1.11	18.29	2081.07	4.56
Median	180.00	372.00	715.00	395.50	577.50	0.00	20.00	2360.00	5.30
Mode	180.00	380.00	0.00	0.00	1135.40	0.00	20.00	2320.00	5.30
Standard Deviation	18.17	70.73	227.85	395.77	377.99	1.88	3.80	807.11	2.87
Lowest	137.00	158.00	0.00	0.00	57.00	0.00	10.00	0.00	0.00
Highest	225.00	600.00	1010.00	1168.00	1574.30	7.80	25.00	2661.00	10.90
Sum	29,942.99	60,493.00	114,285.63	63,414.57	109,011.35	183.49	3036.00	345,457.00	757.10

*W = water (kg/m³); *C = cement (kg/m³); *F-A = fine aggregate (kg/m³); *WA = water absorption (%), NCA (kg/m³), RCA (kg/m³), SP (kg/m³), Size (mm).

2.2. Machine Learning Algorithms

2.2.1. Bagging Algorithm

Bagging, also called bootstrap aggregating, is the structuring of this algorithm in such a way that the ML approaches used in both regression and classification can enhance their firmness and accuracy. It is usually used to lessen the difference between the actual and projected outcomes. Bagging can be used with any method; however, it is most typically used with decision tree approaches. It is also regarded as one of the model averaging technique's special situations. Bagging is a parallel ensemble ML strategy that uses Supplemental Data in the training stage to explain the variance of predicted models. Each element has the same chance of presenting in the new data collection. Variation in the training set has no effect on predictive power. The complete process of the bagging model in the flowchart can be seen in Figure 3.

2.2.2. Artificial Neural Network (ANN)

ANNs are referred to as neural networks (NNs), and they refer to the accruing system that is stimulated by the biological NNs that underpin human brains. ANN is based on a network of units or nodes that are connected to each other, referred to as artificial neurons. The function and structure of neurons are mirror images of the brain. The said neurons absorb a signal prior to functioning and can signal the neuron connected to them. The initial number represents a "signal" at a connection, and each neuron's output is listed by various non-linear functions from the complete inputs. The edges are the connections. Edges, like neurons, typically have a weight that adjusts as learning progresses. The weight is adjusted in response to the strength of the signals at the link. If the aggregate signal travels via a neuron, it may have an entry, such as a processed signal. Typically, neurons are organized in layers. Each layer has a unique purpose associated with its outputs. These

layers act as a conduit for signals to move from the first (input layer) to the last (output layer). The mathematical description of an ANN is shown in Equation (1)

$$O_j = f \sum (w_{ij} I_i + b) \tag{1}$$

where O_j is the model output, w_{ij} denotes the related weight that is changed on a per-epoch basis, I_i denotes the input data, and b denotes the bias. It is worth noting that the hidden layer and output neuron may be processed by feeding them into an activation function f . Figure 4 depicts a schematic representation of a typical ANN architecture.

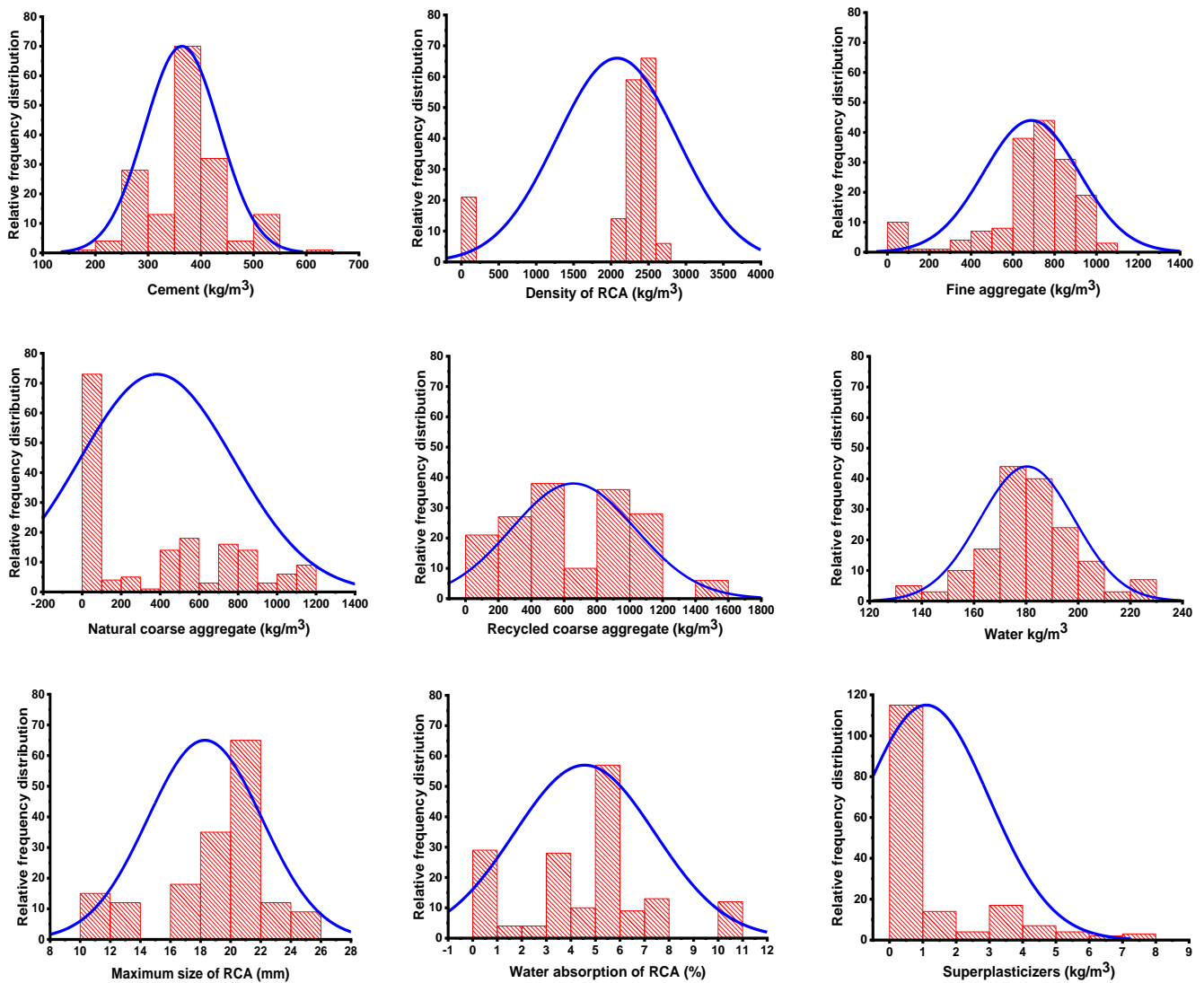


Figure 1. Distribution of relative frequency of the variables used to run the models.

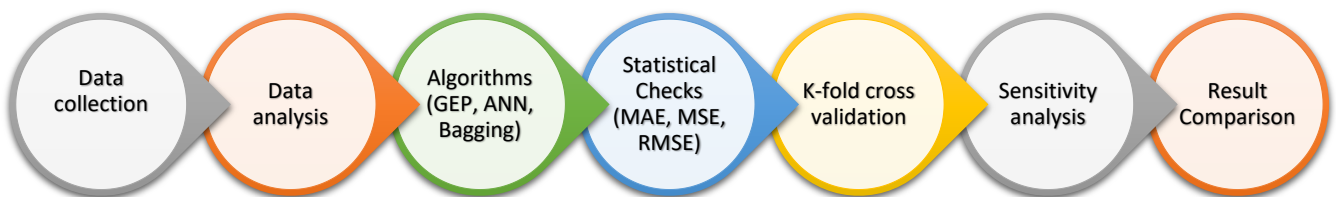


Figure 2. Flowchart of the research.

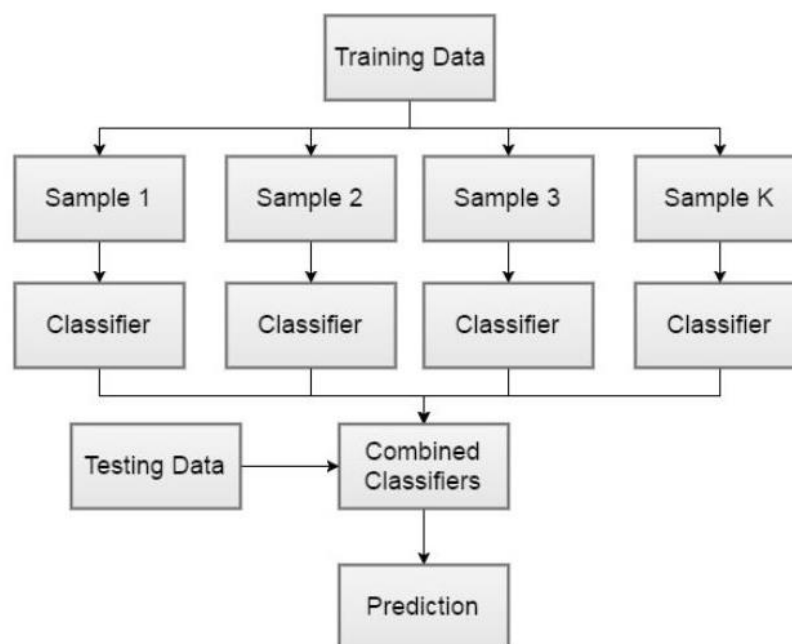


Figure 3. Flowchart of the bagging regressor with the complete execution process.

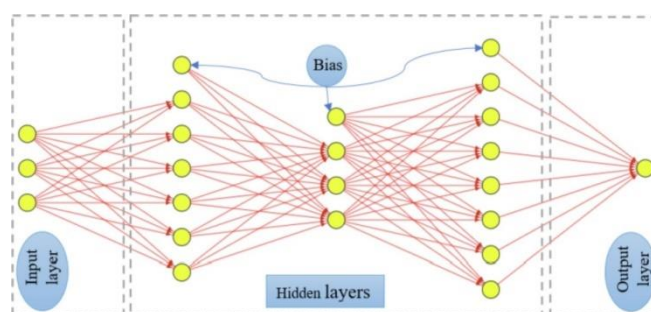


Figure 4. Architecture of artificial neural network [63]. Reprinted with permission from Ref. [63]. Copyright 2022 Elsevier.

2.2.3. Gene Expression Programming (GEP)

GEP is a type of evolutionary algorithm that is frequently used in conjunction with genetic programming. Computer programming is viewed as a complex structure like a tree that adapts and changes the same way that biological organisms do by substituting their geometry, compositions, and sizes. The GEP computer program was embedded in fixed-length simple linear chromosomes. Thus, GEP is a genotype–phenotype system that utilizes the genome to maintain and convey genetic information and a sophisticated phenotype to traverse and adapt to its environment. The GEP is composed of a number of components: terminal, function, control variable, fitness function, and the terminate condition. Ferreira introduced GEP in 2006 as a modified form of genetic programming (GP) based on the evolutionary population theory. A unique constraint in GEP was that only one gene needed to be passed to the next generation; there was no need to replicate and mutate the entire structure because all changes occur inside a linear and basic structure. Additionally, GEP establishes individuals through only one chromosome carrying a number of genes that are subsequently classed as head or tail. Each GEP gene comprises a length with a fixed variable that contains terminal sets and arithmetic operations. There is an unambiguous relationship between the chromosome symbol and the genetic code operator’s matching terminal. The complete execution process for the model using GEP is depicted in Figure 5.

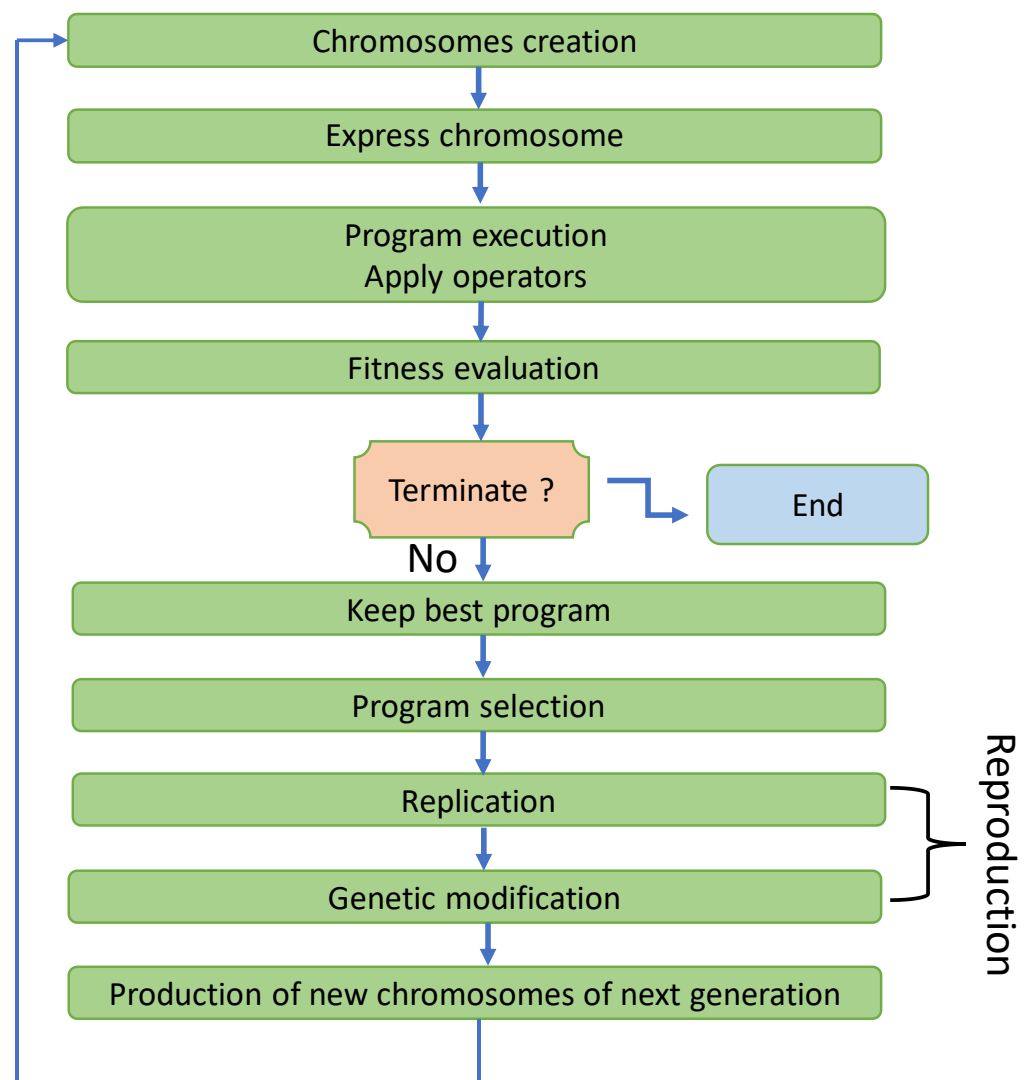


Figure 5. Flowchart indicating the executing process of gene expression programming.

3. Results and Analysis

3.1. ANN Model Outcome

The investigation of the real and projected data for the STS of RA-based concrete using the ANN model is depicted in Figure 6. The ANN technique generates reasonably precise findings with a little variation among the real and anticipated values. With an R^2 score of 0.86, the model is reasonably precise in forecasting the obtained results. The distribution of experimental results (targets), expected outcomes, and error values for the ANN's model are shown in Figure 7. For the testing set, the highest, minimum, and average results of the values were determined to be 1.1, 0.08, and 0.32 MPa, respectively. However, 2.94 percent of error values were up to 0.1 MPa, 52.94 percent of the error's data were between 0.1 and 0.3 MPa, and 41.1 percent exceeded 0.3 MPa.

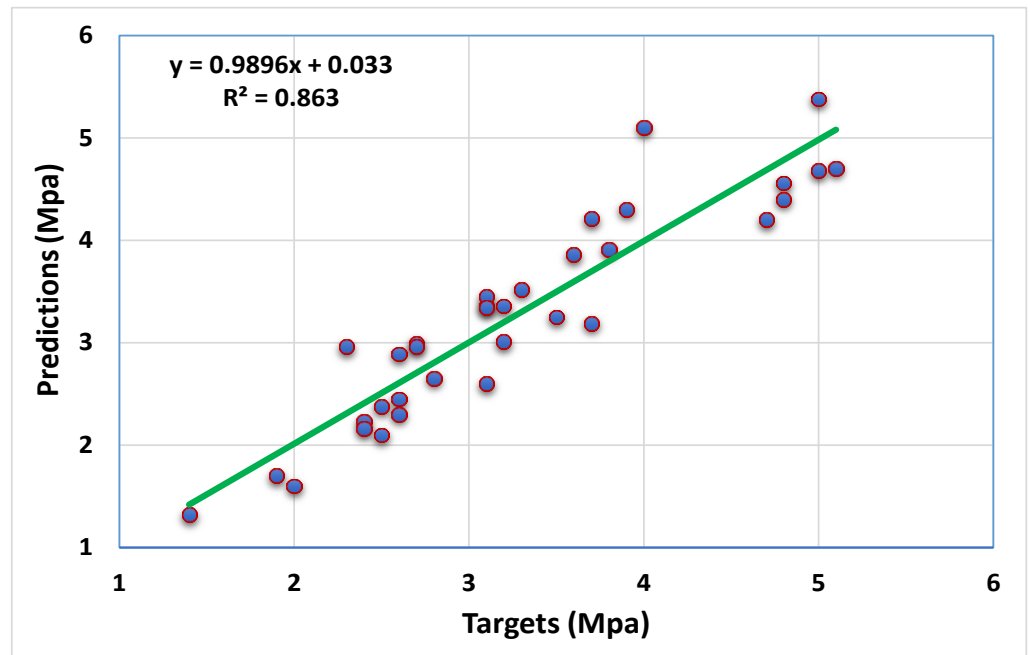


Figure 6. Analysis representing the relationship between the real and forecasted outcomes of ANN model.

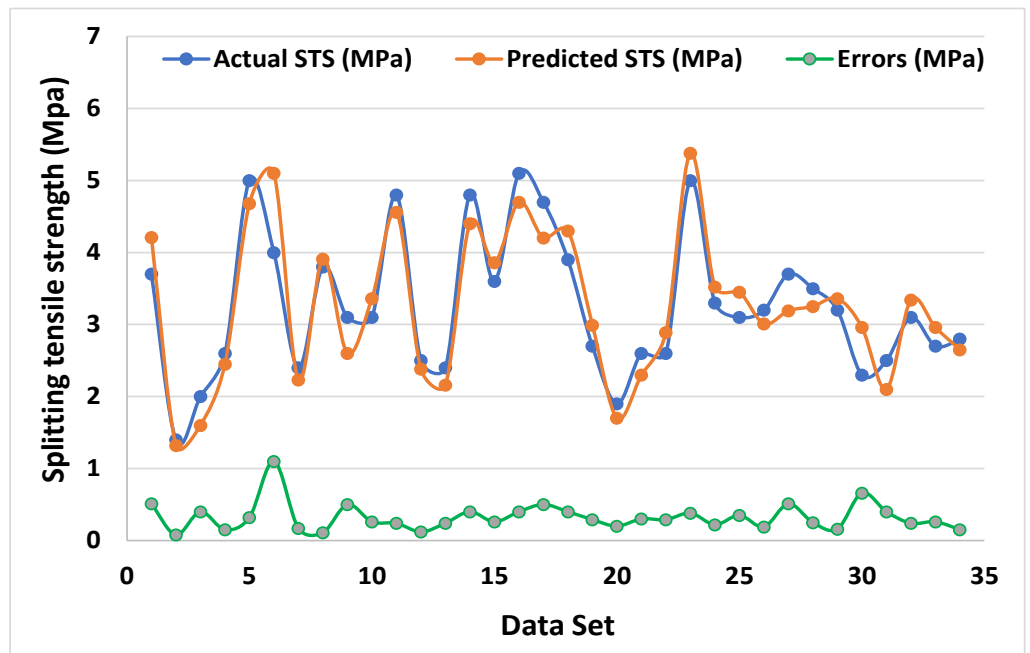


Figure 7. Representation of the error distribution between the real and forecasted outputs for the GEP model.

3.2. GEP Model Outcome

The STS of RA-based concrete for the GEP model statistical evaluation of actual and predicted data is shown in Figure 8. The GEP approach produces results with a decent level of accuracy and a minimal variance between the actual and real results. The R^2 score of 0.88 is the reflection of a reasonably better precision level in predicting the results. Figure 9 illustrates the distribution of targeted results, anticipated results, and errors for the GEP model. The maximum, lower, and average values for the test set were noted to be 1.1, 0,

and 0.25 MPa, respectively. However, 17.64 percent of the error's data were greater than 0.1 MPa, 35.29 percent were between 0.1 and 0.3 MPa, and 26.47 percent exceeded 0.3 MPa.

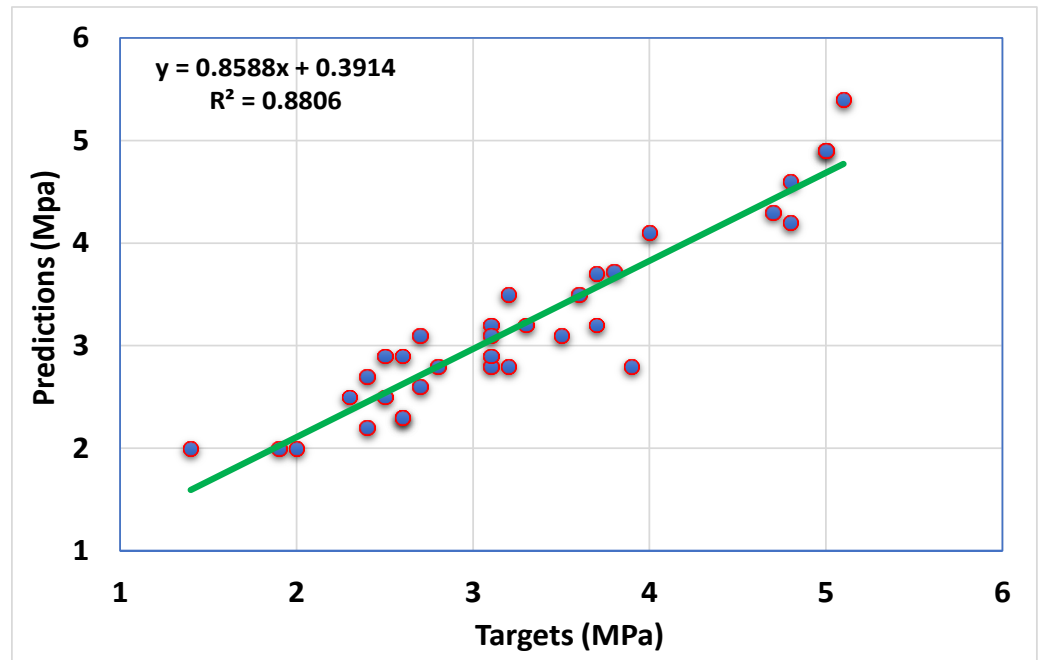


Figure 8. Analysis indicating the relationship between the real and forecasted outcomes using the GEP model.

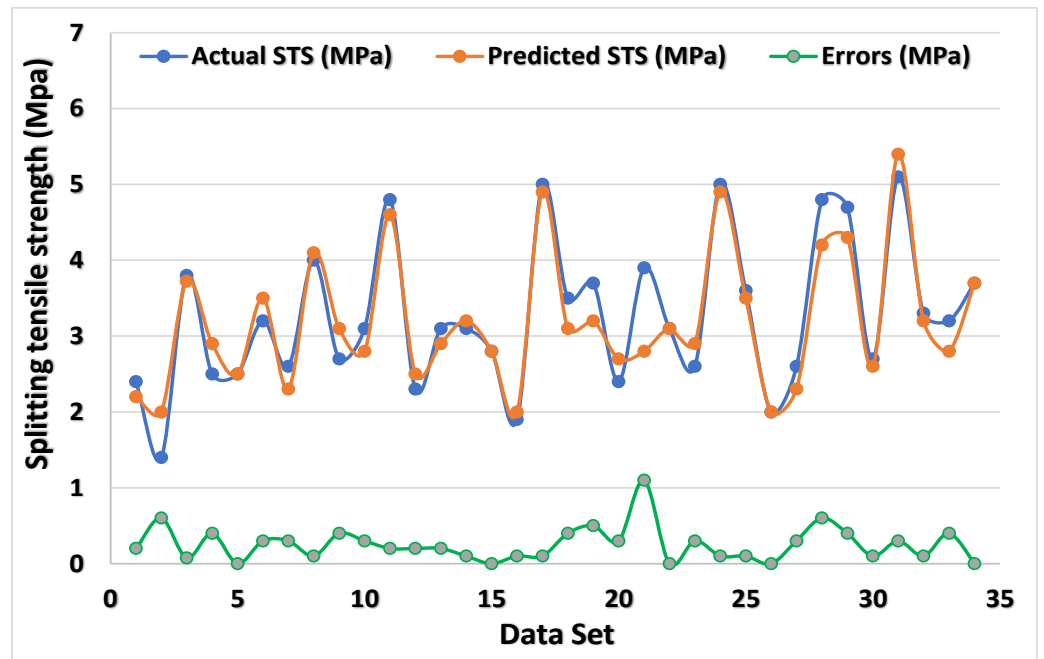


Figure 9. Representation of the error distribution among the real and forecasted outputs for GEP model.

3.3. Bagging Model Outcome

Figures 10 and 11 compare the actual and expected outputs of the bagging model. Figure 10 shows the correlation between the real and predicted results, which gives the R^2 value of 0.95, showing that the result (predicted) of the bagging model is more accurate than the GEP and ANN models. The dispersal of experimental results, anticipated values,

and the results of the error values for the bagging model is depicted in Figure 11. The testing set's maximum, lower, and average values were 0.45, 0, and 0.18 MPa, respectively. However, 14.70% of error values were less than 0.1 MPa, 61.76 percent were between 0.1 and 0.3 MPa, and only 8.82 percent of error values were more than 0.3 MPa. These low values of the errors further support the bagging model's high accuracy when related to the GEP and ANN models.

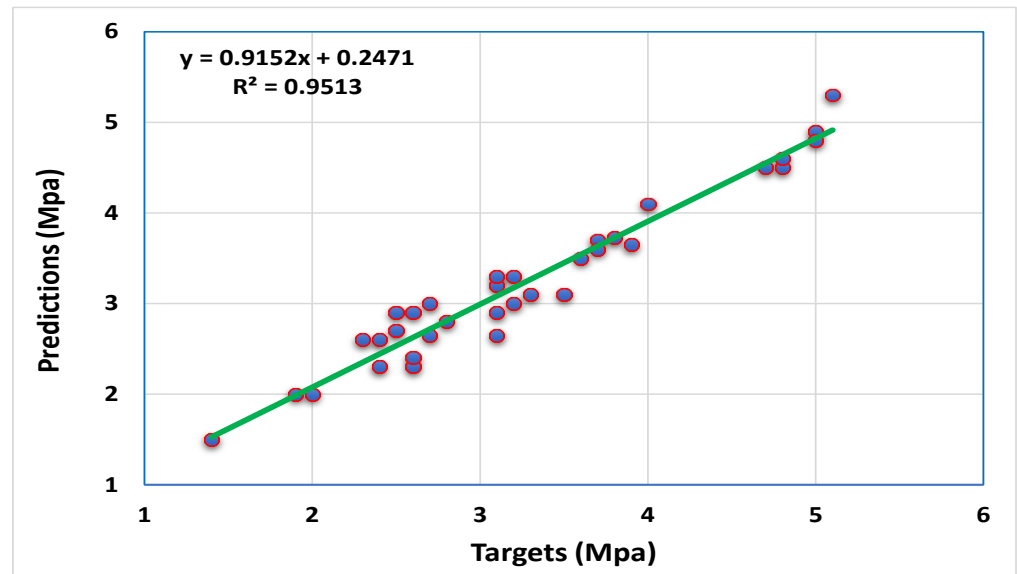


Figure 10. Analysis illustrates the relationship between the real and forecasted outcomes using the bagging model.

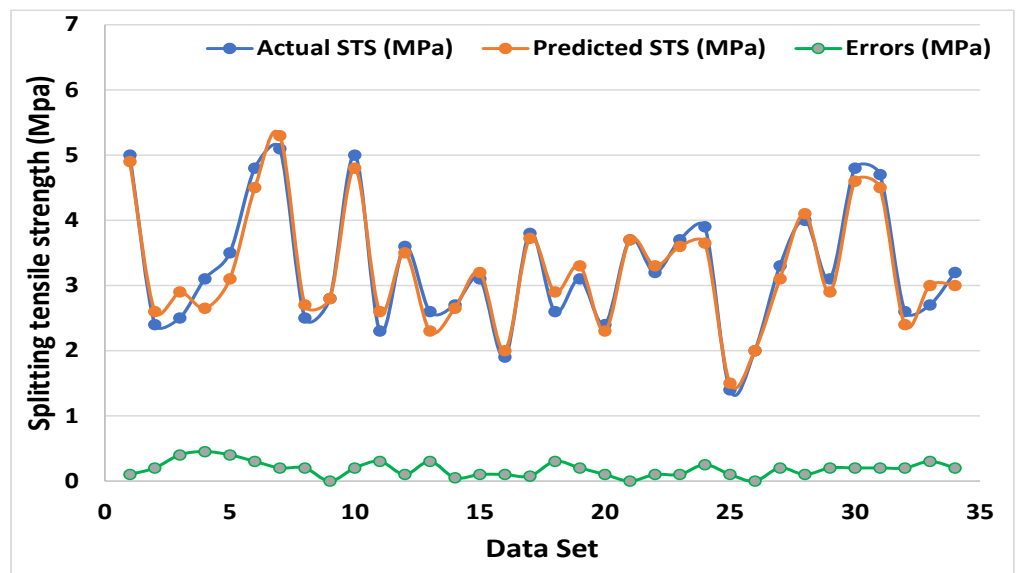


Figure 11. Representation of the error distribution between the real and forecasted outcomes for the GEP model.

4. Cross-Validation (CV) Approach

Cross-validation is a resampling technique that employs different subsets of the data to test and train a model over time. It is primarily utilized in situations where the objective is prediction, and the user wishes to determine the accuracy with which a predictive model will function in practice. To validate the model, a k-fold cross-validation process is typically used, in which the required data are randomly distributed and split into ten groups. Nine

groups must be allocated for training and one for model validation. Additionally, the technique must be repeated ten times to achieve an average output. This exhaustive procedure of k-fold cross-validation leads to the models' great accuracy. Additionally, statistical checks in the form of error evaluations (MSE, MAE, and RMSE) were performed, as demonstrated in Table 2. The models' reaction to prediction was also evaluated using statistical analysis, as demonstrated in the equations below (Equations (2)–(4)).

$$RMSE = \sqrt{\frac{\sum_{i=1}^n (ex_i - mo_i)^2}{n}} \quad (2)$$

$$MAE = \frac{\sum_{i=1}^n |ex_i - mo_i|}{n} \quad (3)$$

$$RMSE = \sqrt{\frac{\sum_{i=1}^n (\bar{ex}_i - \bar{mo}_i)^2}{n}} \quad (4)$$

where ex_i , mo_i , \bar{ex}_i , \bar{mo}_i , and n are experimental, predicted, mean experimental, mean predicted values, and the number of samples, respectively.

Table 2. CV outcomes for both employed models.

K-Fold	GEP			Bagging			ANN		
	MAE	RMSE	R ²	MAE	RMSE	R ²	MAE	RMSE	R ²
1	0.93	0.97	0.06	0.51	0.70	0.08	0.92	1.15	0.61
2	0.73	0.90	0.20	0.67	0.86	0.62	0.83	1.09	0.13
3	0.40	0.70	0.91	0.58	0.68	0.77	0.48	0.73	0.77
4	0.83	1.17	0.28	1.01	1.05	0.93	0.91	1.19	0.35
5	0.10	0.13	0.88	0.46	0.26	0.94	0.14	0.17	0.45
6	0.37	0.53	0.22	0.22	0.33	0.05	0.40	0.55	0.37
7	1.13	1.15	0.56	0.62	0.68	0.24	1.19	1.20	0.74
8	0.73	1.02	0.29	0.72	0.71	0.57	0.78	1.11	0.06
9	0.80	0.82	0.33	0.54	0.61	0.88	0.87	0.87	0.57
10	0.20	0.42	0.85	1.05	0.94	0.9	0.28	0.50	0.44

As seen in Table 2, R², MAE, and RMSE were utilized to determine the CV of each employed model for its output. Additionally, the results of employed AI approaches (GEP, ANN, bagging) used demonstrated variation. The fewer error levels in the bagging model, the higher the R² value, showing that the bagging model has a greater level of precision than the GEP and ANN.

Additionally, as indicated in Table 3, appropriate checks for MAE and RMSE were performed on the GEP, ANN, and bagging techniques. The smaller error indicates a greater coefficient correlation value (R²).

Table 3. Statistical evaluation for STS.

ML Approaches	MAE (MPa)	MSE (MPa)	RMSE (MPa)
Gene expression programming (GEP)	0.252	0.114	0.337
Bagging regressor (BR)	0.183	0.046	0.215
Artificial neural network (ANN)	0.315	0.141	0.375

The R², MAE, MSE, and RMSE coefficients were investigated for the evaluation of the CV and their distributions for GEP, ANN, and bagging models. The bagging model with the result of minimum error value and a high R² value is the indication of high accuracy in predicting outcomes. The higher, minimum, and average R² results for the GEP model

were 0.91, 0.06, and 0.46, respectively. The bagging model's maximum, minimum, and average R^2 results were 0.77, 0.06, and 0.45, respectively, while these values for the ANN model were 0.94, 0.05, and 0.60, respectively.

5. Sensitivity Analysis

This approach refers to the effect of variables on the prediction of the STS of RA concrete, as illustrated in Figure 12. The variables have a substantial impact on the output anticipation. The GEP software directly gives the contribution level of each variable. The dataset was arranged in an Excel file for executing the model. The GEP software gives different information, including the percent contribution of all input parameters. The statistic indicates that cement contributed the most (30.65 percent), while NCA and RA contributed 24.3 percent and 16.2 percent, respectively. However, the remaining variables (fine aggregate, water, superplasticizers, coarse aggregate size, RCA density, and RCA water absorption) had the least effect on the prediction of the STS of RA-based concrete.

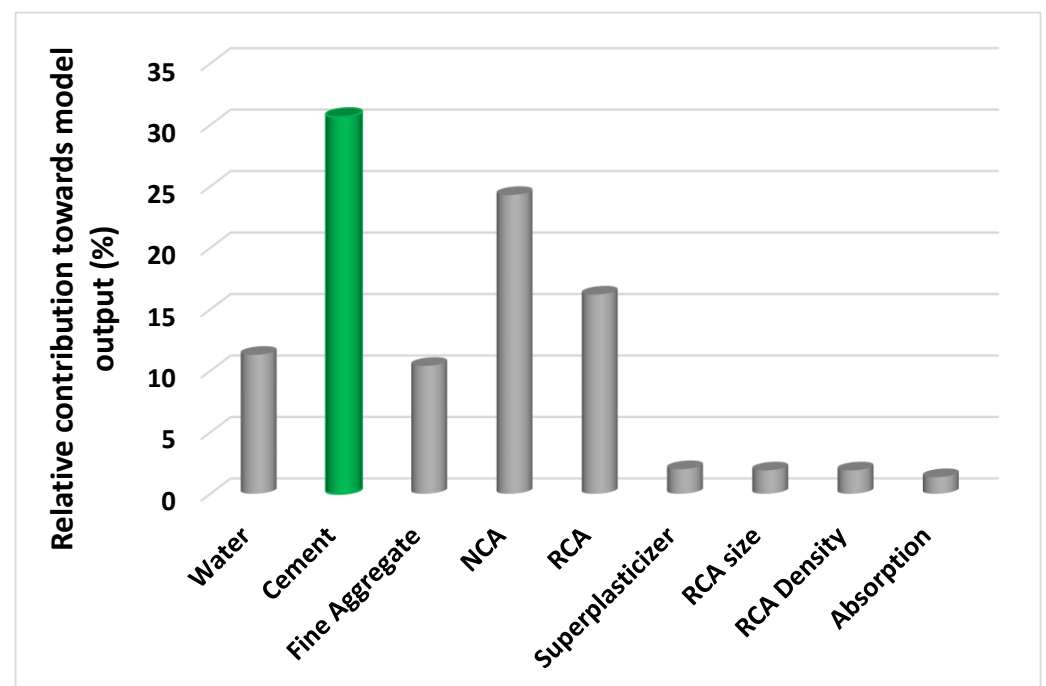


Figure 12. Result of the analysis illustrates the contribution level of variables toward the anticipation of splitting tensile strength.

6. Discussion

This study demonstrates the utility of two distinct machine learning algorithms for estimating the STS of RA-based concrete. The utilization of RA in concrete plays a vital role in achieving sustainable concrete. This approach not only helps in reducing the waste on the earth but also contributes toward a balanced economy, protection of natural resources, and reducing energy consumption. The graphical representation of the numerous parameters that relate to sustainability is depicted in Figure 13.

The GEP algorithm's purpose is to construct a type of model that reliably predicts the results of a targeted variable, for which the GEP makes use of various genres. In supervised learning, bagging is used to minimize both bias and variation. It is forecasted on the premise that learners produce in a sequential fashion. All successive learners, with the exception of the initial learner, are created from preceding learners. In a way, weak learners become better. By contrast, bagging is a technique for randomly selecting data points from a training set with replacement; that is, individual data points may be chosen many times. Following the generation of numerous data samples, these weak models are trained individually, and depending on the task at hand (for example, regression or classification),

the average or majority of those predictions results in a more accurate estimate. The forecast performance of all the algorithms was compared to determine which one was the superior predictor. The bagging model's result was more precise, with an R^2 value of 0.95 versus 0.88 for the GEP model and 0.86 for the ANN model. Additionally, the performance of the GEP, ANN, and bagging models was investigated using a statistical approach and the CV technique. When error levels are minimal, the model performs well. However, evaluating and recommending the ideal ML approach for forecasting results (outcomes) across several topics is challenging, as model behavior is largely dependent on dataset and input variables. In contrast, ensemble machine learning algorithms frequently exploit the weak type of learner by creating multiple models (sub-models) which can be properly trained on data and optimized for the highest R^2 value. The representation of R^2 values for bagging sub-models is depicted in Figure 14. Moreover, the literature shows that bagging models outperform other machine learning algorithms in terms of accuracy. Additionally, the sensitivity analysis was run to determine the effect of each input parameter on the projected STS. The model's performance may be influenced by the parameters used for running the models and the dataset. The sensitivity analysis identifies which input parameters have the greatest impact on the predicted result.

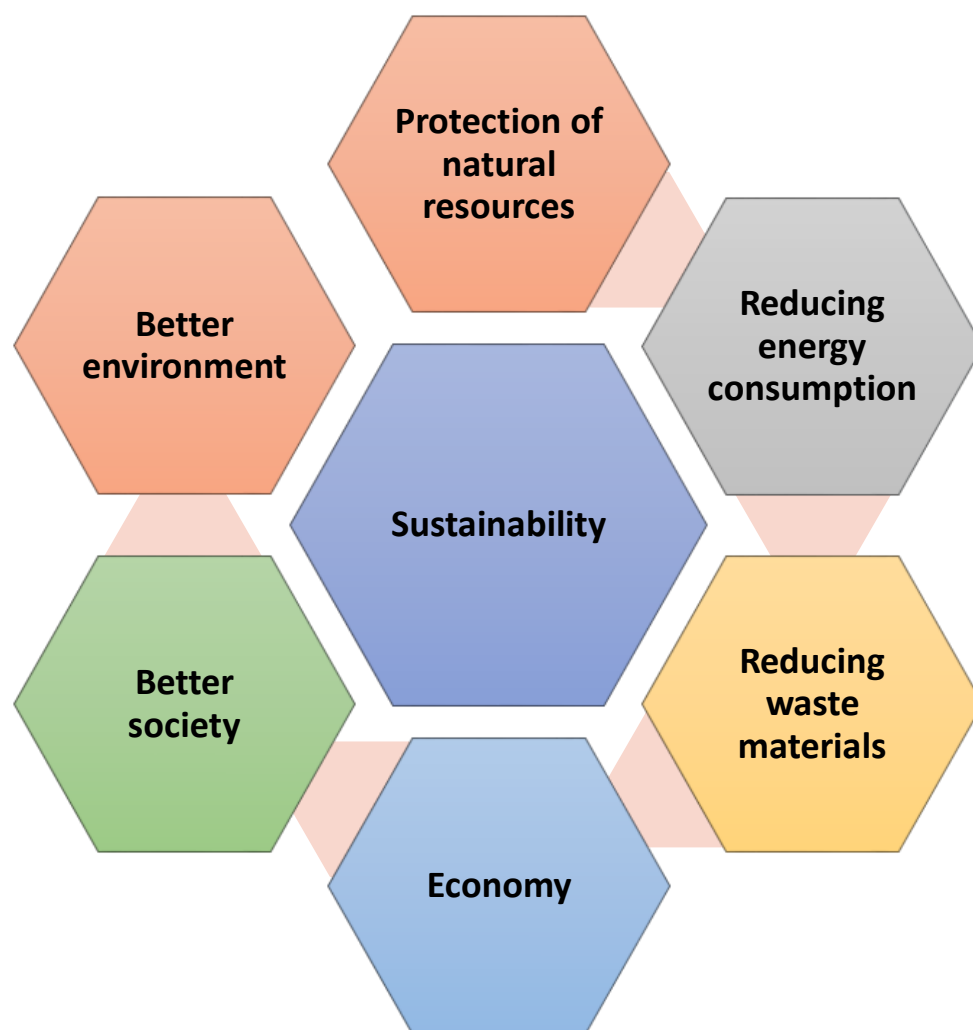


Figure 13. Schematic representation of the improvements in various aspects by achieving sustainability.

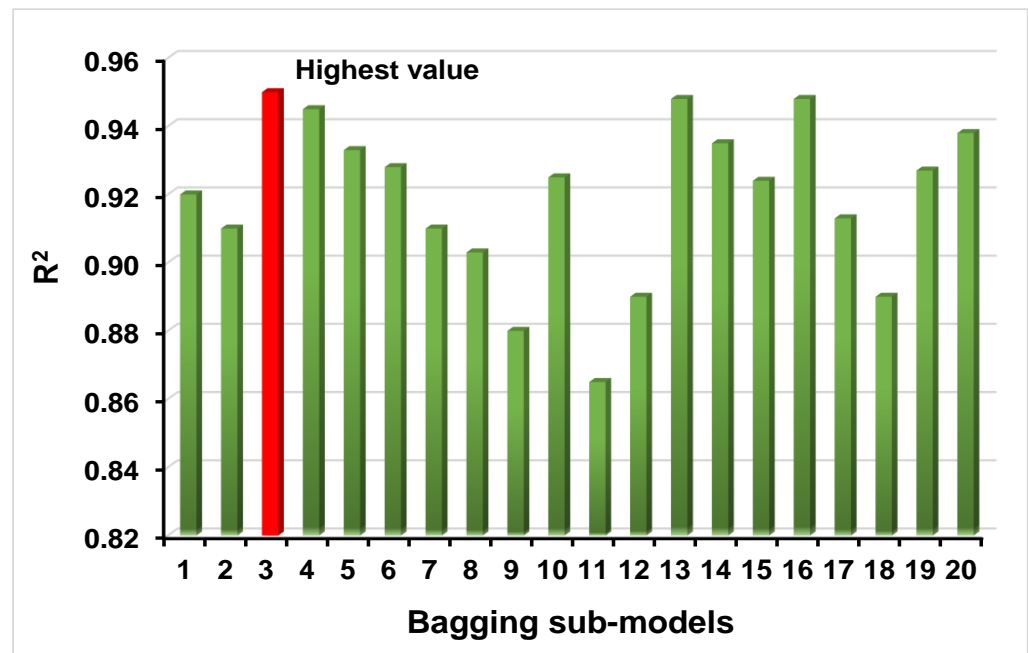


Figure 14. Result of bagging sub-models indicating the coefficient of determination values for each model.

7. Conclusions

The goal of this research was to demonstrate how artificial intelligence (AI) techniques can be used to forecast the strength (STS) of concrete composed of recycled aggregates (RAs). The STS of RA-based concrete was forecasted using GEP, ANN, and bagging regressor (BR) approaches. The following are conclusions:

1. The BR model shows an effective result toward the prediction of the STS of concrete than the GEP and ANN techniques, as demonstrated by a higher R^2 value and a lower result of the errors. GEP, ANN, and BR models were found to have R^2 values of 0.88, 0.86, and 0.95, respectively.
2. Statistical approach/analysis and the cross-validation technique further proved that all the employed techniques (GEP, ANN, and BR) operate satisfactorily. Moreover, these checks demonstrated that the bagging model outperformed the GEP and ANN models in terms of performance.
3. Analysis of sensitivity revealed that the major input variable (cement) contributed at a high level (30.65%) toward the prediction of the STS of RA-based concrete, while another variable (water absorption of RA) contributed the least (1.35%) toward the required output.
4. AI techniques provide more precise forecasting of material strength qualities without consuming time for sample casting and testing in the laboratory.
5. It is recommended that other AI methodologies be adapted to match their predictive accuracy. Additionally, future studies should increase the number of data points by conducting experiments, experimental/field tests, and numerical-type studies utilizing alternative methodologies (e.g., Monte Carlo simulation). Moreover, environmental variables (e.g., high temperature and humidity) could be included as variables to improve the models' response.

Supplementary Materials: The following supporting information can be downloaded at: <https://www.mdpi.com/article/10.3390/cryst12050569/s1>, The data set used for running the models has been added as a supplementary material with the file name of Data set.

Author Contributions: Y.Z.: conceptualization, resources, investigation, methodology, validation, writing—review and editing. A.A.: conceptualization, software, supervision, writing—original draft. W.A.: data curation, methodology, validation, writing—review and editing. N.I.V.: funding acquisition, investigation, project administration, visualization, writing—review and editing. A.M.M.: methodology, formal analysis, writing—review and editing. D.F.: resources, validation, writing—review and editing. All authors have read and agreed to the published version of the manuscript.

Funding: The research was partially funded by the Ministry of Science and Higher Education of the Russian Federation under the strategic academic leadership program “Priority 2030” (Agreement 075-15-2021-1333 dated 30 September 2021).

Institutional Review Board Statement: Not applicable.

Informed Consent Statement: Not applicable.

Data Availability Statement: The data used in the study is available within the study.

Acknowledgments: The authors acknowledge the support of the Ministry of Science and Higher Education of the Russian Federation under the strategic academic leadership program “Priority 2030” (Agreement 075-15-2021-1333 dated 30 September 2021).

Conflicts of Interest: The authors declare no conflict of interest.

References

1. Choi, Y.; Yuan, R.L. Experimental relationship between splitting tensile strength and compressive strength of GFRC and PFRC. *Cem. Concr. Res.* **2005**, *35*, 1587–1591. [[CrossRef](#)]
2. Jin, L.; Yu, W.; Du, X. Size effect on static splitting tensile strength of concrete: Experimental and numerical studies. *J. Mater. Civ. Eng.* **2020**, *32*, 04020308. [[CrossRef](#)]
3. Ahmad, W.; Farooq, S.H.; Usman, M.; Khan, M.; Ahmad, A.; Aslam, F.; Yousef, R.A.; Abduljabbar, H.A.; Sufian, M.J.M. Effect of coconut fiber length and content on properties of high strength concrete. *Materials* **2020**, *13*, 1075. [[CrossRef](#)] [[PubMed](#)]
4. Yang, H.; Liu, L.; Yang, W.; Liu, H.; Ahmad, W.; Ahmad, A.; Aslam, F.; Joyklad, P.J.C.S.i.C.M. A comprehensive overview of geopolymer composites: A bibliometric analysis and literature review. *Case Stud. Constr. Mater.* **2021**, *16*, e00830. [[CrossRef](#)]
5. Zhang, B.; Ahmad, W.; Ahmad, A.; Aslam, F.; Joyklad, P. A scientometric analysis approach to analyze the present research on recycled aggregate concrete. *J. Build. Eng.* **2021**, *46*, 103679. [[CrossRef](#)]
6. Li, X.; Qin, D.; Hu, Y.; Ahmad, W.; Ahmad, A.; Aslam, F.; Joyklad, P. A systematic review of waste materials in cement-based composites for construction applications. *J. Build. Eng.* **2022**, *45*, 103447. [[CrossRef](#)]
7. Ahmad, W.; Ahmad, A.; Ostrowski, K.A.; Aslam, F.; Joyklad, P.; Zajdel, P.J.M. Application of advanced machine learning approaches to predict the compressive strength of concrete containing supplementary cementitious materials. *Materials* **2021**, *14*, 5762. [[CrossRef](#)] [[PubMed](#)]
8. Khan, M.; Cao, M.; Xie, C.; Ali, M. Efficiency of basalt fiber length and content on mechanical and microstructural properties of hybrid fiber concrete. *Fatigue Fract. Eng. Mater. Struct.* **2021**, *44*, 2135–2152. [[CrossRef](#)]
9. Cao, M.; Xie, C.; Li, L.; Khan, M. Effect of different PVA and steel fiber length and content on mechanical properties of CaCO₃ whisker reinforced cementitious composites. *Mater. Construcción* **2019**, *69*, e200. [[CrossRef](#)]
10. Xie, C.; Cao, M.; Khan, M.; Yin, H.; Guan, J. Review on different testing methods and factors affecting fracture properties of fiber reinforced cementitious composites. *Constr. Build. Mater.* **2021**, *273*, 121766. [[CrossRef](#)]
11. Alyousef, R.; Ahmad, W.; Ahmad, A.; Aslam, F.; Joyklad, P.; Alabduljabbar, H. Potential use of recycled plastic and rubber aggregate in cementitious materials for sustainable construction: A review. *J. Clean. Prod.* **2021**, *329*, 129736. [[CrossRef](#)]
12. Shang, M.; Li, H.; Ahmad, A.; Ahmad, W.; Ostrowski, K.A.; Aslam, F.; Joyklad, P.; Majka, T.M. Predicting the Mechanical Properties of RCA-Based Concrete Using Supervised Machine Learning Algorithms. *Materials* **2022**, *15*, 647. [[CrossRef](#)] [[PubMed](#)]
13. Li, L.; Khan, M.; Bai, C.; Shi, K. Uniaxial tensile behavior, flexural properties, empirical calculation and microstructure of multi-scale fiber reinforced cement-based material at elevated temperature. *Materials* **2021**, *14*, 1827. [[CrossRef](#)] [[PubMed](#)]
14. Cao, M.; Mao, Y.; Khan, M.; Si, W.; Shen, S. Different testing methods for assessing the synthetic fiber distribution in cement-based composites. *Constr. Build. Mater.* **2018**, *184*, 128–142. [[CrossRef](#)]
15. Xiao, J.; Li, J.; Zhang, C.J.C. Mechanical properties of recycled aggregate concrete under uniaxial loading. *Cem. Concr. Res.* **2005**, *35*, 1187–1194. [[CrossRef](#)]
16. Marinković, S.; Radonjanin, V.; Malešev, M.; Ignjatović, I. Comparative environmental assessment of natural and recycled aggregate concrete. *Waste Manag.* **2010**, *30*, 2255–2264. [[CrossRef](#)]
17. Tavakoli, M.; Soroushian, P.J.M.J. Strengths of recycled aggregate concrete made using field-demolished concrete as aggregate. *Mater. J.* **1996**, *93*, 178–181.
18. Hansen, T.C.J.M. Recycled aggregates and recycled aggregate concrete second state-of-the-art report developments 1945–1985. *Mater. Struct.* **1986**, *19*, 201–246. [[CrossRef](#)]

19. Bai, G.; Zhu, C.; Liu, C.; Liu, B.J.C. An evaluation of the recycled aggregate characteristics and the recycled aggregate concrete mechanical properties. *Constr. Build. Mater.* **2020**, *240*, 117978. [[CrossRef](#)]
20. Casuccio, M.; Torrijos, M.; Giaccio, G.; Zerbino, R.J.C. Failure mechanism of recycled aggregate concrete. *Constr. Build. Mater.* **2008**, *22*, 1500–1506. [[CrossRef](#)]
21. Sonawane, T.R.; Pimplikar, S.S. Use of recycled aggregate concrete. *IOSR J. Mech. Civ. Eng.* **2013**, *52*, 52–59.
22. Song, H.; Ahmad, A.; Farooq, F.; Ostrowski, K.A.; Maślak, M.; Czarnecki, S.; Aslam, F.J.C. Predicting the compressive strength of concrete with fly ash admixture using machine learning algorithms. *Constr. Build. Mater.* **2021**, *308*, 125021. [[CrossRef](#)]
23. Khan, M.; Cao, M.; Xie, C.; Ali, M.J.S.C. Hybrid fiber concrete with different basalt fiber length and content. *Struct. Concr.* **2021**, *23*, 346–364. [[CrossRef](#)]
24. Cao, M.; Khan, M.; Ahmed, S. Effectiveness of Calcium Carbonate Whisker in Cementitious Composites. *Period. Polytech. Civ. Eng.* **2020**, *64*, 265. [[CrossRef](#)]
25. Khan, M.; Cao, M.; Hussain, A.; Chu, S.J.C. Effect of silica-fume content on performance of CaCO₃ whisker and basalt fiber at matrix interface in cement-based composites. *Constr. Build. Mater.* **2021**, *300*, 124046. [[CrossRef](#)]
26. Lotfi, S.; Eggimann, M.; Wagner, E.; Mróz, R.; Deja, J.J.C. Performance of recycled aggregate concrete based on a new concrete recycling technology. *Constr. Build. Mater.* **2015**, *95*, 243–256. [[CrossRef](#)]
27. Silva, R.; De Brito, J.; Dhir, R.J.C. Tensile strength behaviour of recycled aggregate concrete. *Constr. Build. Mater.* **2015**, *83*, 108–118. [[CrossRef](#)]
28. Dimitriou, G.; Savva, P.; Petrou, M.F.J.C. Enhancing mechanical and durability properties of recycled aggregate concrete. *Constr. Build. Mater.* **2018**, *158*, 228–235. [[CrossRef](#)]
29. Arshad, S.; Sharif, M.B.; Irfan-ul-Hassan, M.; Khan, M.; Zhang, J.-L. Efficiency of supplementary cementitious materials and natural fiber on mechanical performance of concrete. *Arab. J. Sci. Eng.* **2020**, *45*, 8577–8589. [[CrossRef](#)]
30. Yehia, S.; Helal, K.; Abusharkh, A.; Zaher, A.; Istaitiyeh, H. Strength and durability evaluation of recycled aggregate concrete. *Int. J. Concr. Struct. Mater.* **2015**, *9*, 219–239. [[CrossRef](#)]
31. Nagapan, S.; Rahman, I.A.; Asmi, A.; Memon, A.H.; Latif, I. Issues on construction waste: The need for sustainable waste management. In Proceedings of the 2012 IEEE Colloquium on Humanities, Science and Engineering (CHUSER), Kota Kinabalu, Malaysia, 3 December 2012; pp. 325–330.
32. Ye, G.; Yuan, H.; Shen, L.; Wang, H.J.R. Simulating effects of management measures on the improvement of the environmental performance of construction waste management. *Resour. Conserv. Recycl.* **2012**, *62*, 56–63. [[CrossRef](#)]
33. Ahmad, W.; Ahmad, A.; Ostrowski, K.A.; Aslam, F.; Joyklad, P. A scientometric review of waste material utilization in concrete for sustainable construction. *Case Stud. Constr. Mater.* **2021**, *15*, e00683. [[CrossRef](#)]
34. Hu, Y. Minimization management of construction waste. In Proceedings of the 2011 International Symposium on Water Resource and Environmental Protection, Xi'an, China, 20 May 2011; pp. 2769–2772.
35. Ahmad, A.; Chaiyasarn, K.; Farooq, F.; Ahmad, W.; Suparp, S.; Aslam, F.J.B. Compressive strength prediction via gene expression programming (GEP) and artificial neural network (ANN) for concrete containing RCA. *Buildings* **2021**, *11*, 324. [[CrossRef](#)]
36. Ahmad, A.; Farooq, F.; Ostrowski, K.A.; Śliwa-Wieczorek, K.; Czarnecki, S. Application of Novel Machine Learning Techniques for Predicting the Surface Chloride Concentration in Concrete Containing Waste Material. *Materials* **2021**, *14*, 2297. [[CrossRef](#)] [[PubMed](#)]
37. Li, J.; Xiao, H.; Zhou, Y. Influence of coating recycled aggregate surface with pozzolanic powder on properties of recycled aggregate concrete. *Constr. Build. Mater.* **2009**, *23*, 1287–1291. [[CrossRef](#)]
38. Ozbakkaloglu, T.; Gholampour, A.; Xie, T. Mechanical and Durability Properties of Recycled Aggregate Concrete: Effect of Recycled Aggregate Properties and Content. *J. Mater. Civ. Eng.* **2018**, *30*, 04017275. [[CrossRef](#)]
39. Xiao, J.; Li, W.; Poon, C. Recent studies on mechanical properties of recycled aggregate concrete in China—A review. *Sci. China Technol. Sci.* **2012**, *55*, 1463–1480. [[CrossRef](#)]
40. Bui, N.K.; Satomi, T.; Takahashi, H. Improvement of mechanical properties of recycled aggregate concrete basing on a new combination method between recycled aggregate and natural aggregate. *Constr. Build. Mater.* **2017**, *148*, 376–385. [[CrossRef](#)]
41. Nagataki, S.; Gokce, A.; Saeki, T. Effects of Recycled Aggregate Characteristics on Performance Parameters of Recycled Aggregate Concrete. *ACI Symp. Publ.* **2000**, *192*, 53–72. [[CrossRef](#)]
42. Purushothaman, R.; Amirthavalli, R.R.; Karan, L. Influence of Treatment Methods on the Strength and Performance Characteristics of Recycled Aggregate Concrete. *J. Mater. Civ. Eng.* **2015**, *27*, 04014168. [[CrossRef](#)]
43. Zhang, Y.; Luo, W.; Wang, J.; Wang, Y.; Xu, Y.; Xiao, J. A review of life cycle assessment of recycled aggregate concrete. *Constr. Build. Mater.* **2019**, *209*, 115–125. [[CrossRef](#)]
44. Zhu, L.; Dai, J.; Bai, G.; Zhang, F. Study on thermal properties of recycled aggregate concrete and recycled concrete blocks. *Constr. Build. Mater.* **2015**, *94*, 620–628. [[CrossRef](#)]
45. Duan, Z.H.; Kou, S.C.; Poon, C.S. Prediction of compressive strength of recycled aggregate concrete using artificial neural networks. *Constr. Build. Mater.* **2013**, *40*, 1200–1206. [[CrossRef](#)]
46. Silva, R.V.; Neves, R.; de Brito, J.; Dhir, R.K. Carbonation behaviour of recycled aggregate concrete. *Cem. Concr. Compos.* **2015**, *62*, 22–32. [[CrossRef](#)]
47. Mukharjee, B.B.; Barai, S.V. Influence of Nano-Silica on the properties of recycled aggregate concrete. *Constr. Build. Mater.* **2014**, *55*, 29–37. [[CrossRef](#)]

48. Lavado, J.; Bogas, J.; de Brito, J.; Hawreen, A. Fresh properties of recycled aggregate concrete. *Constr. Build. Mater.* **2020**, *233*, 117322. [[CrossRef](#)]
49. Song, Y.; Zhao, J.; Ostrowski, K.A.; Javed, M.F.; Ahmad, A.; Khan, M.I.; Aslam, F.; Kinasz, R. Prediction of Compressive Strength of Fly-Ash-Based Concrete Using Ensemble and Non-Ensemble Supervised Machine-Learning Approaches. *Appl. Sci.* **2022**, *12*, 361. [[CrossRef](#)]
50. Akhtar, A.; Sarmah, A.K. Construction and demolition waste generation and properties of recycled aggregate concrete: A global perspective. *J. Clean. Prod.* **2018**, *186*, 262–281. [[CrossRef](#)]
51. Pradhan, S.; Kumar, S.; Barai, S.V. Multi-scale characterisation of recycled aggregate concrete and prediction of its performance. *Cem. Concr. Compos.* **2020**, *106*, 103480. [[CrossRef](#)]
52. Li, X. Recycling and reuse of waste concrete in China: Part II. Structural behaviour of recycled aggregate concrete and engineering applications. *Resour. Conserv. Recycl.* **2009**, *53*, 107–112. [[CrossRef](#)]
53. Xuan, D.; Zhan, B.; Poon, C.S. Durability of recycled aggregate concrete prepared with carbonated recycled concrete aggregates. *Cem. Concr. Compos.* **2017**, *84*, 214–221. [[CrossRef](#)]
54. Su, M.; Zhong, Q.; Peng, H.; Li, S. Selected machine learning approaches for predicting the interfacial bond strength between FRPs and concrete. *Constr. Build. Mater.* **2021**, *270*, 121456. [[CrossRef](#)]
55. Jin, R.; Chen, Q.; Soboyejo, A.B.O. Non-linear and mixed regression models in predicting sustainable concrete strength. *Constr. Build. Mater.* **2018**, *170*, 142–152. [[CrossRef](#)]
56. Ohemeng, E.A.; Ekolu, S.O.; Quainoo, H.; Kruger, D. Model for predicting compressive strength and elastic modulus of recycled concrete made with treated coarse aggregate: Empirical approach. *Constr. Build. Mater.* **2022**, *320*, 126240. [[CrossRef](#)]
57. Ohemeng, E.A.; Ekolu, S.O.; Quainoo, H. Models for predicting strength properties of recycled concretes made with non-treated CRCAs: Empirical approach. *Constr. Build. Mater.* **2021**, *307*, 124585. [[CrossRef](#)]
58. Amin, M.N.; Iqtidar, A.; Khan, K.; Javed, M.F.; Shalabi, F.I.; Qadir, M.G. Comparison of Machine Learning Approaches with Traditional Methods for Predicting the Compressive Strength of Rice Husk Ash Concrete. *Crystals* **2021**, *11*, 779. [[CrossRef](#)]
59. Dabiri, H.; Kioumars, M.; Kheyroddin, A.; Kandiri, A.; Sartipi, F. Compressive strength of concrete with recycled aggregate; a machine learning-based evaluation. *Clean. Mater.* **2022**, *3*, 100044. [[CrossRef](#)]
60. Kandiri, A.; Sartipi, F.; Kioumars, M. Predicting Compressive Strength of Concrete Containing Recycled Aggregate Using Modified ANN with Different Optimization Algorithms. *Appl. Sci.* **2021**, *11*, 485. [[CrossRef](#)]
61. Dabiri, H.; Rahimzadeh, K.; Kheyroddin, A. A comparison of machine learning- and regression-based models for predicting ductility ratio of RC beam-column joints. *Structures* **2022**, *37*, 69–81. [[CrossRef](#)]
62. Alagundi, S.; Palanisamy, T. Neural network prediction of joint shear strength of exterior beam-column joint. *Structures* **2022**, *37*, 1002–1018. [[CrossRef](#)]
63. Dabiri, H.; Kheyroddin, A.; Faramarzi, A. Predicting tensile strength of spliced and non-spliced steel bars using machine learning- and regression-based methods. *Constr. Build. Mater.* **2022**, *325*, 126835. [[CrossRef](#)]
64. Wu, Z.; Shen, L.; Yu, A.T.W.; Zhang, X. A comparative analysis of waste management requirements between five green building rating systems for new residential buildings. *J. Clean. Prod.* **2016**, *112*, 895–902. [[CrossRef](#)]
65. Javed, M.F.; Farooq, F.; Memon, S.A.; Akbar, A.; Khan, M.A.; Aslam, F.; Alyousef, R.; Alabduljabbar, H.; Rehman, S.K.U. New Prediction Model for the Ultimate Axial Capacity of Concrete-Filled Steel Tubes: An Evolutionary Approach. *Crystals* **2020**, *10*, 741. [[CrossRef](#)]
66. Farooq, F.; Rahman, S.K.U.; Akbar, A.; Khushnood, R.A.; Javed, M.F.; Alyousef, R.; Alabduljabbar, H.; Aslam, F. A comparative study on performance evaluation of hybrid GNP/CNTs in conventional and self-compacting mortar. *Alex. Eng. J.* **2020**, *59*, 369–379. [[CrossRef](#)]
67. Khan, M.A.; Farooq, F.; Javed, M.F.; Zafar, A.; Ostrowski, K.A.; Aslam, F.; Malazdrewicz, S.; Maślak, M. Simulation of Depth of Wear of Eco-Friendly Concrete Using Machine Learning Based Computational Approaches. *Materials* **2022**, *15*, 58. [[CrossRef](#)]
68. Nafees, A.; Javed, M.F.; Khan, S.; Nazir, K.; Farooq, F.; Aslam, F.; Musarat, M.A.; Vatin, N.I. Predictive Modeling of Mechanical Properties of Silica Fume-Based Green Concrete Using Artificial Intelligence Approaches: MLPNN, ANFIS, and GEP. *Materials* **2021**, *14*, 7531. [[CrossRef](#)]
69. Kim, H.-K.; Lim, Y.; Tafesse, M.; Kim, G.M.; Yang, B. Micromechanics-integrated machine learning approaches to predict the mechanical behaviors of concrete containing crushed clay brick aggregates. *Constr. Build. Mater.* **2022**, *317*, 125840. [[CrossRef](#)]
70. Lee, S.-C. Prediction of concrete strength using artificial neural networks. *Eng. Struct.* **2003**, *25*, 849–857. [[CrossRef](#)]
71. Sharafati, A.; Haji Seyed Asadollah, S.B.; Al-Ansari, N. Application of bagging ensemble model for predicting compressive strength of hollow concrete masonry prism. *Ain Shams Eng. J.* **2021**, *12*, 3521–3530. [[CrossRef](#)]
72. Han, T.; Siddique, A.; Khayat, K.; Huang, J.; Kumar, A. An ensemble machine learning approach for prediction and optimization of modulus of elasticity of recycled aggregate concrete. *Constr. Build. Mater.* **2020**, *244*, 118271. [[CrossRef](#)]
73. Abd Elhakam, A.; Mohamed, A.E.; Awad, E. Influence of self-healing, mixing method and adding silica fume on mechanical properties of recycled aggregates concrete. *Constr. Build. Mater.* **2012**, *35*, 421–427. [[CrossRef](#)]
74. Ajdukiewicz, A.; Kliszczewicz, A. Influence of recycled aggregates on mechanical properties of HS/HPC. *Cem. Concr. Compos.* **2002**, *24*, 269–279. [[CrossRef](#)]
75. Fathifazl, G.; Ghani Razaqpur, A.; Burkan Isgor, O.; Abbas, A.; Fournier, B.; Foo, S. Creep and drying shrinkage characteristics of concrete produced with coarse recycled concrete aggregate. *Cem. Concr. Compos.* **2011**, *33*, 1026–1037. [[CrossRef](#)]

76. Chakradhara Rao, M.; Bhattacharyya, S.K.; Barai, S.V. Influence of field recycled coarse aggregate on properties of concrete. *Mater. Struct.* **2011**, *44*, 205–220. [[CrossRef](#)]
77. Pereira, P.; Evangelista, L.; de Brito, J. The effect of superplasticizers on the mechanical performance of concrete made with fine recycled concrete aggregates. *Cem. Concr. Compos.* **2012**, *34*, 1044–1052. [[CrossRef](#)]
78. Butler, L.; West, J.S.; Tighe, S.L. Effect of recycled concrete coarse aggregate from multiple sources on the hardened properties of concrete with equivalent compressive strength. *Constr. Build. Mater.* **2013**, *47*, 1292–1301. [[CrossRef](#)]
79. Thomas, C.; Setién, J.; Polanco, J.A.; Alaejos, P.; Sánchez de Juan, M. Durability of recycled aggregate concrete. *Constr. Build. Mater.* **2013**, *40*, 1054–1065. [[CrossRef](#)]
80. Andreu, G.; Miren, E. Experimental analysis of properties of high performance recycled aggregate concrete. *Constr. Build. Mater.* **2014**, *52*, 227–235. [[CrossRef](#)]
81. Duan, Z.H.; Poon, C.S. Properties of recycled aggregate concrete made with recycled aggregates with different amounts of old adhered mortars. *Mater. Des.* **2014**, *58*, 19–29. [[CrossRef](#)]
82. Pedro, D.; de Brito, J.; Evangelista, L. Performance of concrete made with aggregates recycled from precasting industry waste: Influence of the crushing process. *Mater. Struct.* **2015**, *48*, 3965–3978. [[CrossRef](#)]
83. Limbachiya, M.C.; Leelawat, T.; Dhir, R.K. Use of recycled concrete aggregate in high-strength concrete. *Mater. Struct.* **2000**, *33*, 574. [[CrossRef](#)]
84. Gómez-Soberón, J.M.V. Porosity of recycled concrete with substitution of recycled concrete aggregate: An experimental study. *Cem. Concr. Res.* **2002**, *32*, 1301–1311. [[CrossRef](#)]
85. Etxeberria, M.; Mari, A.R.; Vázquez, E. Recycled aggregate concrete as structural material. *Mater. Struct.* **2007**, *40*, 529–541. [[CrossRef](#)]
86. Kou, S.C.; Poon, C.S.; Chan, D. Influence of Fly Ash as Cement Replacement on the Properties of Recycled Aggregate Concrete. *J. Mater. Civ. Eng.* **2007**, *19*, 709–717. [[CrossRef](#)]
87. Kou, S.C.; Poon, C.S.; Chan, D. Influence of fly ash as a cement addition on the hardened properties of recycled aggregate concrete. *Mater. Struct.* **2008**, *41*, 1191–1201. [[CrossRef](#)]
88. Yang, K.-H.; Chung, H.-S.; Ashour, A.F. Influence of Type and Replacement Level of Recycled Aggregates on Concrete Properties. *ACI Mater. J.* **2008**, *105*, 289–296.
89. Zega, C.J.; Maio, A.A.D. Recycled Concretes Made with Waste Ready-Mix Concrete as Coarse Aggregate. *J. Mater. Civ. Eng.* **2011**, *23*, 281–286. [[CrossRef](#)]